

Sound scattering by nested cylindrically symmetric and linearly invariant anomalies

Sven M. Ivansson¹

¹SE-11529 Stockholm, Sweden

Sven M. Ivansson, SE-11529 Stockholm, Sweden; sven.ivansson@gmail.com

Abstract: Several previous papers have applied the coupled-mode method to assess three-dimensional scattering by cylindrically symmetric anomalies (e.g., seamounts) or anomalies which are invariant in a horizontal direction (e.g., wedges and canyons). Based on a medium discretization with laterally homogeneous rings and strips, an extension to combinations of the two anomaly types has recently been made. For each anomaly, the computations involve recursively determined reflection matrices, which relate the expansion coefficients for incoming and outgoing normal modes. Concerning ring and strip anomalies, the horizontal variation of these expansion coefficients is conveniently described by cylindrical and plane wave functions, respectively. Iterative solution of a linear equation system for the amplitudes of the scattered cylindrical waves from the ring anomalies, involving formulas for transformation between plane and cylindrical waves, allows numerical computation of the field. Within this iterative solution procedure, adaptive numerical integration is used to compute discrete sets of expansion coefficients, resulting from strip-structure interaction, for cylindrical waves incident on the ring anomalies. The present paper develops a further extension, where the ring anomalies need not be disjoint but can be nested within each other and within the strip structure of the medium. Additional translation formulas for cylindrical wave function come into play. Furthermore, the iterates for solution of a pertinent linear equation system for the amplitudes of the scattered cylindrical waves from the ring anomalies are now themselves determined iteratively. The field within a ring anomaly containing other ring anomalies follows by solving a multiple-source problem with the included ring anomalies as (additional) effective sources. Partial waves can be computed to study details of multiple scattering among individual ring and strip anomalies. It can thereby be convenient to use nested ring anomalies with common centre points.

Keywords: wave-function translation, reflection-matrix recursion, mode coupling, partial waves

1. INTRODUCTION

The discrete coupled-mode method, with a horizontal discretization of the medium into laterally homogeneous regions, is extended in [1] to compute the 3D pressure field p in fluid media which include a combination of cylindrically symmetric ring anomalies R and linearly invariant strip anomalies S . The computations are performed iteratively, incorporating successively higher orders of multiple scattering between the ring and strip anomalies. Hence, see [1, Eq. (37)], the successive terms in the field expansion $p = p_R + p_{S,R} + p_{R,S,R} + \dots$ are computed. The initial partial field p_R ignores the strip anomalies. Further scattering by the strip anomalies give rise to additional incident waves on the ring anomalies, with discrete sets of cylindrical-wave expansion coefficients, which can be computed efficiently by adaptive wavenumber integration.

For example, see [1, Fig. 4], it is possible to solve the pertinent Helmholtz equation for 3D underwater sound propagation in a strait with two cylindrically symmetric islands. Figure 1 concerns the same example, but for 50 rather than 25 Hz. The two islands, similar with outer and inner radii 1.6 and 1.0 km, respectively, are centred at $(x, y) = (1, 7)$ and $(1, 14)$ km, respectively, in a Cartesian xy coordinate system for the horizontal plane. Up-sloping strait boundaries appear between $x = -1$ and -4 km, and between $x = 3$ and 6 km. Of course, there are now more propagating modes, six rather than three where the water depth is 200 m. The main characteristics of the fields at 50 and 25 Hz are rather similar, however.

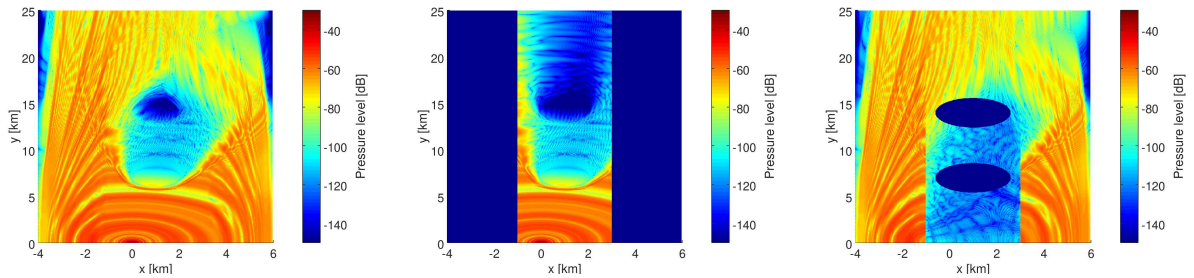


Figure 1: Coupled-mode results, in dB re 1 m, as in [1, Fig. 4(a)-(c)] but for 50 Hz. In particular, the example concerns two islands in a strait. The left panel shows the full field p , while the middle and right panels show partial waves from the iterative solution procedure: p_R (middle), and $p_{S,R}$ (right).

Returning to 25 Hz, Fig. 2 concerns media with modified water depth for $x < -1$ km, 200 m for $x < -3$ km and: constant water depth 200 m for $x < -1$ km (left), cosine-shaped trench between $x = -3$ and -1 km with maximum water depth 300 m (middle), and cosine-shaped ridge between $x = -3$ and -1 km with minimum water depth 100 m (right). Furthermore, the source is moved from $(x, y) = (0, 0)$ km to $(x, y) = (-3, 0)$ km, but it is still at depth 40 m, and the receivers are still at depth 30 m. The down-slope and up-slope parts of the trench cause reduction and enhancement, respectively, of the field strength. Transmission through the ridge is weak for large y , corresponding to grazing-like incidence with strong reflections back. In the ridge case, the field that is incident on the ring anomaly centred at $(1, 14)$ km is thus weak, causing a strong shadow behind it. For the examples in Fig. 2, $N \times 2D$ approximation results (not shown) are rather good.

As clarified in [2], it is possible to approximate the strip anomalies with very large cylindrically symmetric ring anomalies with a common horizontal centre point far away. The original ring anomalies then appear within the corresponding laterally homogeneous rings with large radii. In effect, a structure appears with nested cylindrically symmetric anomalies. The main

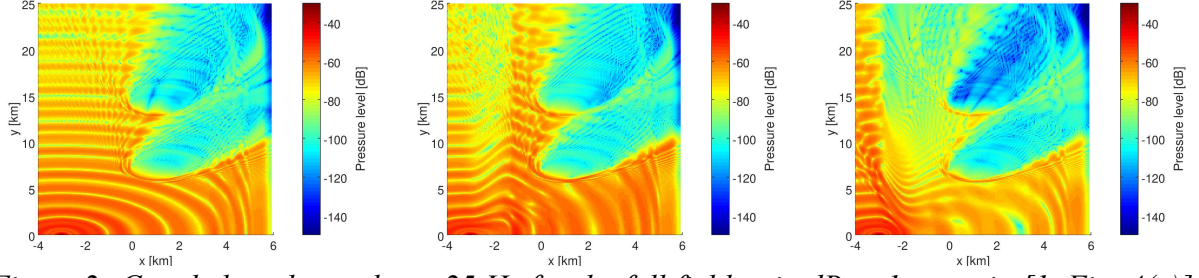


Figure 2: Coupled-mode results at 25 Hz for the full field p , in dB re 1 m, as in [1, Fig. 4(a)] but for modified media as described in the text. In particular, the water depth is 200 m for $x < -1$ km with the exception of a trench (middle panel) or a ridge (right panel) between $x = -3$ and -1 km. The source is now at $(x, y) = (-3, 0)$ km.

purpose of the present paper is to generalize [1] to rather general media with nested cylindrically symmetric anomalies within a strip structure. Section 2 provides the basic equations, Sec. 3 proposes an iterative solution method for the main equation (10), and Sec. 4 indicates how to compute partial waves for multiple scattering among individual ring and strip anomalies. There are no further examples, however, since this generalization of [1] has not yet been implemented on the computer.

2. BASIC EQUATIONS

As in [1], consider a fluid medium and a Cartesian xyz coordinate system with depth z . For a symmetric time-harmonic point source with moment-tensor strength M at $\mathbf{x}_s = (x_s, y_s, z_s)$, the problem is to compute the pressure field $p(\mathbf{x})$ at each point \mathbf{x} . The typically omitted time factor is $\exp(-i\omega t)$, where $\omega > 0$ is angular frequency and t is time. The fluid extends between the finite (computational) depth boundaries $z = z_a(x, y)$ and $z = z_b(x, y) > z_a(x, y)$. These exterior boundaries are locally reacting, such that $p(\mathbf{x})$ satisfies [1, Eq. (1)].

In the present paper, the medium is independent of the horizontal y -coordinate except within J cylindrically symmetric ring anomalies with centre points (x_j, y_j) and outer radii $r_{1,j}$, where $j=1,2,\dots,J$. In contrast to [1], these ring anomalies need not be disjoint but they can be nested within each other. For computations with the discrete coupled-mode method, the medium is discretized into $N_0 + 1$ strips which are parallel to the y -axis. This discretization takes care of possible y -independent strip anomalies. Except for included ring anomalies, each strip is laterally homogeneous. With N_0 vertical interfaces $x_{1,0} < x_{2,0} < \dots < x_{N_0,0}$, strip n covers $x_{n-1,0} < x < x_{n,0}$ for $n=2,3,\dots,N_0$, while strips 1 and $N_0 + 1$ include $x < x_{1,0}$ and $x_{N_0,0} < x$, respectively.

As in [1], ring anomaly j is discretized with $N_j + 1$ horizontal rings, numbered from outside and separated by concentric circles $r_j(x, y) = r_{n,j}$. Local polar coordinates $(r_j(x, y), \phi_j(x, y))$ are centred at (x_j, y_j) in the xy -plane. The $r_{n,j}$, $n = 1, 2, \dots, N_j$, form a decreasing sequence of positive radii. Each ring anomaly j , $j=1,2,\dots,J$, can be within a ring $n_e(j) > 1$ of another ring anomaly denoted $j_e(j) = 1, \dots, J$. Nested chains of ring anomalies can thus be formed, but $n_e(j), j_e(j)$ concern the closest surrounding ring anomaly in a chain. For the outermost ring anomaly j in a chain, $j_e(j) = 0$ and $n_e(j) = 1, 2, \dots, N_0 + 1$ is the strip in which it is contained. Except for included ring anomalies, and other strips than $n_e(j)$ for ring 1 of a ring anomaly j with $j_e(j) = 0$, each ring is laterally homogeneous. The vertical strip and ring interfaces must not intersect. For $n=1,2,\dots,N_0 + 1$, it is convenient to define the sets $J_{n,0} = \{j = 1, 2, \dots, J :$

$n_e(j) = n$ and $j_e(j) = 0$. Moreover, for $j=1,2,\dots,J$, $J_{n,j} = \{j' = 1, 2, \dots, J : n_e(j') = n \text{ and } j_e(j') = j\}$ when $n=2,3,\dots,N_j + 1$, while $J_{1,j} = \{j' = 1, 2, \dots, J : n_e(j') = n_e(j) \text{ and } j_e(j') = j_e(j), \text{ and } j' \neq j\}$. In [1], where all ring anomalies are disjoint, $J_{n,0}$ is simply denoted as J_n . Figure 3 gives an illustration, cf. [1, Fig. 1].

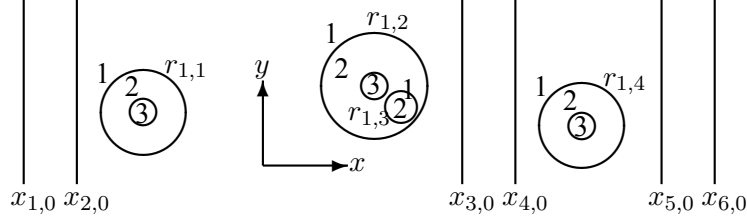


Figure 3: The horizontal xy -plane with a strip structure and four ring anomalies together with their ring radii and ring numbers. In this case, $N_0 = 6$, $J = 4$, $N_1 = N_2 = N_4 = 2$, and $N_3 = 1$. Furthermore, $j_e(1) = j_e(2) = j_e(4) = 0$ and $j_e(3) = 2$, while $n_e(1) = n_e(2) = 3$, $n_e(3) = 2$, and $n_e(4) = 5$. $J_{1,0} = J_{2,0} = J_{4,0} = J_{6,0} = J_{7,0} = \emptyset$, while $J_{3,0} = \{1, 2\}$ and $J_{5,0} = \{4\}$. $J_{2,1} = J_{3,1} = J_{3,2} = J_{1,3} = J_{2,3} = J_{1,4} = J_{2,4} = J_{3,4} = \emptyset$, while $J_{1,1} = \{2\}$, $J_{1,2} = \{1\}$, and $J_{2,2} = \{3\}$. The sound source can be anywhere in the medium, within one of the horizontal ring anomalies or outside all of them.

Densities $\rho_{n,j}(z)$, sound speeds $c_{n,j}(z)$, Lamé parameters $\lambda_{n,j}(z)$, as well as modal horizontal wavenumbers $k_{m,n,j}$ and normalized (n.b.) mode functions $Z_{m,n,j}(z)$, are as in [1]. This is true for the depth boundaries $z_{a;n,j}, z_{b;n,j}$, the admittance values $Y_{a;n,j}, Y_{b;n,j}$, and the depth intervals $I_{n,j}$ as well. Of course, for each j and n , these quantities are only relevant outside possible interior ring anomalies within the corresponding strip or ring. For $j' \in J_{n,j}$, $\rho_{1,j'}(z) = \rho_{n,j}(z)$, $c_{1,j'}(z) = c_{n,j}(z)$, etc. This is true for all $j=0,1,2,\dots,J$.

With the following clarification, j_s and n_s for the source are also as in [1]. Unless $j_s = 0$, j_s and $n_s (> 1)$ concern the smallest ring anomaly containing the source.

For $j=0,1,2,\dots,J$ and $n=1,2,\dots,N_j + 1$, the row vectors $\Phi_{n,j}(\mathbf{x})$ and $\Psi_{n,j}(\mathbf{x})$ are as in [1]. Of course, $\nu=0,1,\dots$ still denotes azimuthal order, $\sigma=e,o$ indicates even,odd parity (for $\nu = 0$ only $\sigma = e$), and κ is still the wavenumber parameter pertaining to Fourier transformation with respect to y . For $n=1,2,\dots,N_0 + 1$, the diagonal matrices $\hat{\mathbf{E}}_n$ are also as in [1]. The mode-coupling matrices $\mathbf{F}_{n,j}, \mathbf{G}_{n,j}, \bar{\mathbf{F}}_{n,j}, \bar{\mathbf{G}}_{n,j}$, and $\mathbf{L}_{n,j}$ remain unchanged too.

With $J_{n,0}$ replacing J_n , the field representation [1, Eq. (8)] is still valid. Immediately outside ring anomaly $j=1,\dots,J$, [1, Eq. (10)] holds with $n = 1$. Within ring $n=2,\dots,N_j + 1$ of ring anomaly $j=1,\dots,J$ (but outside possibly included other ring anomalies there),

$$\begin{aligned} p(\mathbf{x}) = & \delta_{j_s j} \delta_{n n_s} \sum_m a_{m,s} Z_{m,n_s,j_s}(z) H_0^{(1)}(k_{m,n_s,j_s} r_s(x, y)) + \sum_{j' \in J_{n,j}} \Psi_{1,j'}(\mathbf{x}) \cdot \mathbf{b}_{1,j'} \\ & + \Phi_{n,j}(\mathbf{x}) \cdot (\bar{\mathbf{a}}_{n,j} + \bar{\mathbf{a}}_{n,j}^L + \bar{\mathbf{a}}_{n,j}^R) + \Psi_{n,j}(\mathbf{x}) \cdot (\mathbf{b}_{n,j} + \mathbf{b}_{n,j}^L + \mathbf{b}_{n,j}^R). \end{aligned} \quad (1)$$

Here, $\bar{\mathbf{a}}_{n,j} = \{(\bar{a}_{n,j})_{m,\nu,\sigma}\}$, $\bar{\mathbf{a}}_{n,j}^L = \{(\bar{a}_{n,j}^L)_{m,\nu,\sigma}\}$, $\bar{\mathbf{a}}_{n,j}^R = \{(\bar{a}_{n,j}^R)_{m,\nu,\sigma}\}$, and $\mathbf{b}_{n,j} = \{(b_{n,j})_{m,\nu,\sigma}\}$, $\mathbf{b}_{n,j}^L = \{(b_{n,j}^L)_{m,\nu,\sigma}\}$, $\mathbf{b}_{n,j}^R = \{(b_{n,j}^R)_{m,\nu,\sigma}\}$, are column vectors. The coefficient vectors $\bar{\mathbf{a}}_{n,j}^L$ and $\mathbf{b}_{n,j}^L$ represent contributions originating from source and anomalies outside the disk $r_j(x, y) < r_{n-1,j}$. For $n \leq N_j$, $\bar{\mathbf{a}}_{n,j}^R$ and $\mathbf{b}_{n,j}^R$ represent contributions originating from source and ring anomalies inside the disk $r_j(x, y) < r_{n,j}$, while $\bar{\mathbf{a}}_{N_j+1,j}^R = \mathbf{b}_{N_j+1,j}^R = \mathbf{0}$. Apparently, $\bar{\mathbf{a}}_{2,j}^L$ and $\mathbf{b}_{2,j}^L$ are determined by $\mathbf{a}_{1,j}$ from [1, Eq. (10) with $n=1$]. Moreover, $\mathbf{b}_{N_j+1,j} = \mathbf{b}_{N_j+1,j}^L = \mathbf{0}$ are boundary conditions. As in [1], δ is the Kronecker delta and $r_s(x, y) = |(x, y) - (x_s, y_s)|$.

Next, counterparts of the wave-transformation relations [1, Eqs. (13) and (17)] are formulated. Consider ring anomaly $j=1,2,...,J$. When $j_e(j) = j' > 0$,

$$\Psi_{n',j'}(\mathbf{x}) = \Phi_{1,j}(\mathbf{x}) \cdot \mathbf{Q}_{1,j,n',j'} \quad \text{and} \quad \Phi_{n',j'}(\mathbf{x}) = \Phi_{1,j}(\mathbf{x}) \cdot \mathbf{P}_{1,j,n',j'} \quad (2)$$

are valid with $n' = n_e(j) > 1$, where the first relation requires that $|(x, y) - (x_j, y_j)| < |(x_{j'}, y_{j'}) - (x_j, y_j)|$. The elements $(Q_{1,j,n',j'})_{m,\nu,\sigma;m',\nu',\sigma'}$ and $(P_{1,j,n',j'})_{m,\nu,\sigma;m',\nu',\sigma'}$ of the matrices $\mathbf{Q}_{1,j,n',j'}$ and $\mathbf{P}_{1,j,n',j'}$, respectively, agree with those of $\mathbf{Q}_{j,j'}$, as given in [3, (Eqs. (11)-(12))], with the following changes: 1) replace the modal wavenumbers $k_{m,1}$ by $k_{m,1,j} = k_{m,n',j'}$, 2) concerning $\mathbf{Q}_{1,j,n',j'}$, replace $r_{1,j'}$ by $r_{n',j'}$, and 3) concerning $\mathbf{P}_{1,j,n',j'}$, replace the Hankel functions $H_{\nu-\nu'}^{(1)}$ and $H_{\nu+\nu'}^{(1)}$ by the corresponding Bessel functions $J_{\nu-\nu'}$ and $J_{\nu+\nu'}$, respectively, and replace division with $H_{\nu'}^{(1)}(k_{m,1}r_{1,j'})$ by multiplication with $H_{\nu'}^{(1)}(k_{m,n',j'}r_{n'-1,j'})$. This follows from [1, Eq. (12)] and [4, Eq. (5.10)].

When $n > 1$ and $J_{n,j}$ is nonempty for ring anomaly $j=1,2,...,J$, consider an included ring anomaly $j' \in J_{n,j}$. Applying [1, Eq. (12)] and [4, Eq. (5.11)], with matrices $\hat{\mathbf{H}}_{n,j}$ as in [3],

$$\Psi_{1,j'}(\mathbf{x}) = \Phi_{n,j}(\mathbf{x}) \cdot \hat{\mathbf{H}}_{n,j}^{-1} \cdot \mathbf{Q}_{n,j,1,j'} \quad \text{and} \quad \Psi_{1,j'}(\mathbf{x}) = \Psi_{n,j}(\mathbf{x}) \cdot \hat{\mathbf{H}}_{n,j}^{-1} \cdot \mathbf{P}_{n,j,1,j'} \quad (3)$$

are valid for $|(x, y) - (x_j, y_j)| < |(x_{j'}, y_{j'}) - (x_j, y_j)|$ and $|(x, y) - (x_j, y_j)| > |(x_{j'}, y_{j'}) - (x_j, y_j)|$, respectively. The elements $(Q_{n,j,1,j'})_{m,\nu,\sigma;m',\nu',\sigma'}$ and $(P_{n,j,1,j'})_{m,\nu,\sigma;m',\nu',\sigma'}$ of the matrices $\mathbf{Q}_{n,j,1,j'}$ and $\mathbf{P}_{n,j,1,j'}$, respectively, agree with those of $\mathbf{Q}_{j,j'}$, as given in [3, (Eqs. (11)-(12))], with the following changes: 1) replace $k_{m,1}$ by $k_{m,n,j} = k_{m,1,j'}$, 2) concerning $\mathbf{Q}_{n,j,1,j'}$, replace $r_{1,j}$ by $r_{n,j}$, and 3) concerning $\mathbf{P}_{n,j,1,j'}$, replace $H_{\nu-\nu'}^{(1)}$ and $H_{\nu+\nu'}^{(1)}$ by $J_{\nu-\nu'}$ and $J_{\nu+\nu'}$, respectively, and replace division with $H_{\nu}^{(1)}(k_{m,1}r_{1,j})$ by multiplication with $H_{\nu}^{(1)}(k_{m,n,j}r_{n-1,j})$.

With $J_{n,0}$ replacing J_n , [1, Eqs. (20)-(22)] are still valid. Concerning the ring-anomaly computations for each $j=1,2,...,J$, the reflection matrices $\bar{\mathbf{R}}_{n,j}$, mentioned at the end of [1, Sec. 2.3], are now not only needed for $j = j_s$ and $n=1,2,...,n_s$ but also for $n=1,2,...,\max\{n' > 1 : J_{n',j} \neq \emptyset\}$. This is so, since ring anomalies within ring anomaly j act as (additional) effective sources. The counterpart of [1, Eq. (20)] becomes

$$\mathbf{b}_{n,j}^L = \mathbf{R}_{n,j} \cdot \hat{\mathbf{H}}_{n,j} \cdot \bar{\mathbf{a}}_{n,j}^L, \quad \mathbf{b}_{n,j} = \mathbf{R}_{n,j} \cdot \mathbf{a}_{n,j}, \quad \bar{\mathbf{a}}_{n,j}^R = \bar{\mathbf{R}}_{n,j} \cdot \hat{\mathbf{H}}_{n,j} \cdot \mathbf{b}_{n,j}^R, \quad \bar{\mathbf{a}}_{n,j} = \bar{\mathbf{R}}_{n,j} \cdot \bar{\mathbf{b}}_{n,j} \quad (4)$$

for $n = 2, 3, \dots, N_j + 1$. Here, by a generalization of [3, Eqs. (29) and (32)] to the present context, using Eqs. (3),

$$\mathbf{a}_{n,j} = \hat{\mathbf{H}}_{n,j} \cdot \bar{\mathbf{a}}_{n,j} - \delta_{j_s j} \delta_{nn_s} \frac{iM\omega^2}{4\lambda_{n_s,j_s}(z_s)} \Psi_{n_s,j_s}^T(\mathbf{x}_s) + \sum_{j' \in J_{n,j}} \mathbf{Q}_{n,j,1,j'} \cdot \mathbf{b}_{1,j'} \quad (5)$$

$$\bar{\mathbf{b}}_{n,j} = \hat{\mathbf{H}}_{n,j} \cdot \mathbf{b}_{n,j} - \delta_{j_s j} \delta_{nn_s} \frac{iM\omega^2}{4\lambda_{n_s,j_s}(z_s)} \Phi_{n_s,j_s}^T(\mathbf{x}_s) + \sum_{j' \in J_{n,j}} \mathbf{P}_{n,j,1,j'} \cdot \mathbf{b}_{1,j'}. \quad (6)$$

The incoming waves upon ring anomaly $j=1,2,...,J$ appear as $\Phi_{1,j}(\mathbf{x}) \cdot \mathbf{a}_{1,j}$. With $\mathbf{a}_{1,j}^S$ and $\mathbf{a}_{1,j}^0$ still according to [1, Eqs. (25)-(26)],

$$\mathbf{a}_{1,j} = \delta_{j_s j_e(j)} \delta_{n_s n_e(j)} \mathbf{a}_{1,j}^0 + \sum_{j' \in J_{1,j}} \mathbf{Q}_{j,j'} \cdot \mathbf{b}_{1,j'} + \delta_{0j_e(j)} \mathbf{a}_{1,j}^S + (1 - \delta_{0j_e(j)}) \mathbf{a}_{1,j}^R, \quad (7)$$

which represents an extension of [1, Eq. (24)], note that $J_{1,j} = \{j' \in J_{n_e(j),j_e(j)} : j' \neq j\}$. Concerning $\mathbf{a}_{1,j}^R$, note the difference to $\bar{\mathbf{a}}_{n,j}^R$ and $\mathbf{b}_{n,j}^R$, with the superscript R for $\mathbf{a}_{1,j}^R$ indicating ring-anomaly interaction. When $j_e(j) \neq 0$, and hence $n_e(j) > 1$, Eqs. (1) and (2) yield

$$\begin{aligned} \mathbf{a}_{1,j}^R &= \mathbf{P}_{1,j,n_e(j),j_e(j)} \cdot \left(\bar{\mathbf{a}}_{n_e(j),j_e(j)} + \bar{\mathbf{a}}_{n_e(j),j_e(j)}^L + \bar{\mathbf{a}}_{n_e(j),j_e(j)}^R \right) \\ &+ \mathbf{Q}_{1,j,n_e(j),j_e(j)} \cdot \left(\mathbf{b}_{n_e(j),j_e(j)} + \mathbf{b}_{n_e(j),j_e(j)}^L + \mathbf{b}_{n_e(j),j_e(j)}^R \right). \end{aligned} \quad (8)$$

Application of the reflection-matrix operator $\mathbf{R}_{1,j}$ subsequently gives the following slight modification of [1, Eq. (27)]:

$$\mathbf{b}_{1,j} = \mathbf{b}_{1,j}^0 + \mathbf{R}_{1,j} \cdot \mathbf{a}_{1,j} . \quad (9)$$

Now, $\Psi_{1,j}(\mathbf{x}) \cdot \mathbf{b}_{1,j}^0$ provides the scattered waves originating not only from the source when $j = j_s \neq 0$, but also from ring anomalies $j' \in J_{n,j}$ for $n=2,3,\dots,N_j + 1$. In matrix form, Eq. (9) appears as

$$\mathbf{b}_1 = \mathbf{b}_1^0(\mathbf{b}_1) + \mathbf{R}_1 \cdot (\mathbf{a}_1^0 + \mathbf{Q} \cdot \mathbf{b}_1 + \mathbf{a}_1^S(\mathbf{b}_1) + \mathbf{a}_1^R(\mathbf{b}_1)) , \quad (10)$$

Modifications compared to [1, Eq. (28)] are that \mathbf{Q} is now a $J \times J$ block matrix with block j, j' given by $(1 - \delta_{jj'}) \delta_{n_e(j)} \delta_{n_e(j')} \delta_{j_e(j)} \delta_{j_e(j')} \mathbf{Q}_{j,j'}$, while \mathbf{b}_1^0 , \mathbf{a}_1^0 , \mathbf{a}_1^S , and the additional \mathbf{a}_1^R are column vectors with J parts with part j given by $\mathbf{b}_{1,j}^0$, $\delta_{j_s j_e(j)} \delta_{n_s n_e(j)} \mathbf{a}_{1,j}^0$, $\delta_{0 j_e(j)} \mathbf{a}_{1,j}^S$, and $(1 - \delta_{0 j_e(j)}) \mathbf{a}_{1,j}^R$, respectively. As indicated by the notation, all of \mathbf{b}_1^0 , \mathbf{a}_1^S , and \mathbf{a}_1^R now depend on \mathbf{b}_1 . These dependencies are linear, with possible constant terms arising directly from the source (when $j_s \neq 0$, $j_s = 0$, and $j_s \neq 0$ with $J_{n,j_s} \neq \emptyset$ for some $n=2,\dots,N_{j_s} + 1$, respectively).

3. NUMERICAL SOLUTION

The amended version of [1, Eq. (29)] becomes

$$\mathbf{b}_1 = (\mathbf{I} - \mathbf{R}_1 \cdot \mathbf{Q})^{-1} \cdot [\mathbf{b}_1^0(\mathbf{b}_1) + \mathbf{R}_1 \cdot (\mathbf{a}_1^0 + \mathbf{a}_1^S(\mathbf{b}_1) + \mathbf{a}_1^R(\mathbf{b}_1))] . \quad (11)$$

For trial \mathbf{b}_1^0 , \mathbf{a}_1^S , and \mathbf{a}_1^R , it is suitable to compute $(\mathbf{I} - \mathbf{R}_1 \cdot \mathbf{Q})^{-1} \cdot [\mathbf{b}_1^0 + \mathbf{R}_1 \cdot (\mathbf{a}_1^0 + \mathbf{a}_1^S + \mathbf{a}_1^R)]$ by expanding $(\mathbf{I} - \mathbf{R}_1 \cdot \mathbf{Q})^{-1}$ in geometric series, which corresponds precisely to the iterative computation method of [3, Sec. III B]. The computation of $\mathbf{a}_1^S(\mathbf{b}_1)$ for a trial \mathbf{b}_1 proceeds according to [1, Sec. 3.1 and Appendix A]. Of course, $J_{n,0}$ thereby replaces J_n in [1, Eqs. (30)-(31)] When $j_s > 0$, $n_{s,0}$ in [1, Sec. 3.1] now equals $n_e(j')$ where j' , with $j_e(j') = 0$, is the outermost ring anomaly in the nesting chain containing ring anomaly j_s . Recall that, for each κ , [1, Appendix A] shows how to compute $\bar{\mathbf{a}}_{n,0}^L$ and $\mathbf{b}_{n,0}^R$ recursively by *two* passes of stabilized back-propagation throughout the strip structure to pick up contributions from the left and from the right, respectively. The coefficient vectors $\mathbf{b}_{n,0}^L$ and $\bar{\mathbf{a}}_{n,0}^R$ follow from [1, Eqs. (20)].

To compute $\mathbf{a}_1^R(\mathbf{b}_1)$ for a trial \mathbf{b}_1 , first note that substitution of the reflection-matrix expressions for $\mathbf{b}_{n,j}$ and $\bar{\mathbf{a}}_{n,j}$ from Eqs. (4) into Eqs. (5)-(6) provides an equation system with the solution, for $j=1,2,\dots,J$ and $n=2,3,\dots,N_j + 1$,

$$\begin{aligned} \mathbf{a}_{n,j} = & (\mathbf{I} - \bar{\mathbf{S}}_{n,j} \cdot \mathbf{S}_{n,j})^{-1} \cdot \left[-\delta_{j_s j} \delta_{nn_s} \frac{iM\omega^2}{4\lambda_{n_s,j_s}(z_s)} \cdot (\Psi_{n_s,j_s}^T(\mathbf{x}_s) \right. \\ & \left. + \bar{\mathbf{S}}_{n,j} \cdot \Phi_{n_s,j_s}^T(\mathbf{x}_s)) + \sum_{j' \in J_{n,j}} (\mathbf{Q}_{n,j,1,j'} + \bar{\mathbf{S}}_{n,j} \cdot \mathbf{P}_{n,j,1,j'}) \cdot \mathbf{b}_{1,j'} \right] \end{aligned} \quad (12)$$

$$\begin{aligned} \bar{\mathbf{b}}_{n,j} = & (\mathbf{I} - \mathbf{S}_{n,j} \cdot \bar{\mathbf{S}}_{n,j})^{-1} \cdot \left[-\delta_{j_s j} \delta_{nn_s} \frac{iM\omega^2}{4\lambda_{n_s,j_s}(z_s)} \cdot (\Phi_{n_s,j_s}^T(\mathbf{x}_s) \right. \\ & \left. + \mathbf{S}_{n,j} \cdot \Psi_{n_s,j_s}^T(\mathbf{x}_s)) + \sum_{j' \in J_{n,j}} (\mathbf{P}_{n,j,1,j'} + \mathbf{S}_{n,j} \cdot \mathbf{Q}_{n,j,1,j'}) \cdot \mathbf{b}_{1,j'} \right] , \end{aligned} \quad (13)$$

where $\mathbf{S}_{n,j} = \hat{\mathbf{H}}_{n,j} \cdot \mathbf{R}_{n,j}$ and $\bar{\mathbf{S}}_{n,j} = \hat{\mathbf{H}}_{n,j} \cdot \bar{\mathbf{R}}_{n,j}$. Of course, $\mathbf{b}_{n,j}$ and $\bar{\mathbf{a}}_{n,j}$ subsequently follow from Eqs. (4).

For a ring anomaly j with $j_e(j) = 0$, Eq. (7) provides $\mathbf{a}_{1,j}$ for a trial \mathbf{b}_1 . Formally defining $\bar{\mathbf{a}}_{1,j} = \bar{\mathbf{a}}_{1,j}^L = \bar{\mathbf{a}}_{1,j}^R = \mathbf{0}$, it is then easy to adapt [1, Appendix A], which concerns the $\bar{\mathbf{a}}_{n,0}^L$ and

$\mathbf{b}_{n,0}^R$, to computation of the coefficient vectors $\bar{\mathbf{a}}_{n,j}^L$ and $\mathbf{b}_{n,j}^R$. The adaptation involves replacement of N_0 by N_j , subscripts $,_0$ by $,_j$, matrices \mathbf{K}_n by \mathbf{I} , and matrices $\hat{\mathbf{E}}_n$ by $\hat{\mathbf{H}}_{n,j}$. Of course, the computations now concern particular ν, σ pairs rather than particular κ , Eqs. (4) are used instead of [1, Eqs. (20)], and the matrices $\mathbf{L}_{n,j}$ are formally obtained from [1, Eq. (A.2)] by setting $\kappa=0$ (and replacing the subscripts $,_0$ with $,_j$). There are two passes of stabilized back-propagation throughout the rings of ring anomaly j to pick up contributions from the source, when $j_s = j$, and from ring anomalies j' with $j_e(j') = j$. The coefficient vectors $\mathbf{b}_{n,j}^L$ and $\bar{\mathbf{a}}_{n,j}^R$ then follow from Eq. (4). For a ring anomaly j' with $j_e(j') = j$, $\mathbf{a}_{1,j'}^R$ and $\mathbf{a}_{1,j'}$ for the trial \mathbf{b}_1 subsequently follow from Eqs. (8) and (7). The adapted [1, Appendix A] then provides the coefficient vectors $\bar{\mathbf{a}}_{n,j'}^L$ and $\mathbf{b}_{n,j'}^R$, needed to compute $\mathbf{a}_{1,j''}^R$ and $\mathbf{a}_{1,j''}$ for a ring anomaly j'' with $j_e(j'') = j'$. Continuing in this way, to handle the nesting chains of ring anomalies, $\mathbf{a}_{1,j}^R$ and $\mathbf{a}_{1,j}$ for the trial \mathbf{b}_1 follow for all $j=1,2,\dots,J$.

The determination of $\mathbf{b}_{1,j}^0$ for a trial \mathbf{b}_1 proceeds in a similar way, but independently for each $j=1,2,\dots,J$. This time, the computations according to the adapted [1, Appendix A] are initiated with $\mathbf{a}_{1,j}$ temporarily set to zero, and the resulting $\mathbf{b}_{1,j}^R$ provides the desired $\mathbf{b}_{1,j}^0$.

One possibility to extend the iterative solution procedure from [1, Sec. 3.2] to solution of Eq. (11) is as follows. Corresponding to the trial $\mathbf{a}_1^S = \mathbf{0}$, let $\mathbf{b}_1^{(0)}$ solve $\mathbf{b}_1^{(0)} = (\mathbf{I} - \mathbf{R}_1 \cdot \mathbf{Q})^{-1} \cdot [\mathbf{b}_1^0(\mathbf{b}_1^{(0)}) + \mathbf{R}_1 \cdot (\mathbf{a}_1^0 + \mathbf{a}_1^R(\mathbf{b}_1^{(0)}))]$. For $l=0,1,\dots$, let $\mathbf{b}_1^{(l+1)}$ solve

$$\mathbf{b}_1^{(l+1)} = \mathbf{b}_1^{(0)} + (\mathbf{I} - \mathbf{R}_1 \cdot \mathbf{Q})^{-1} \cdot [\mathbf{b}_1^{0-}(\mathbf{b}_1^{(l+1)} - \mathbf{b}_1^{(0)}) + \mathbf{R}_1 \cdot (\mathbf{a}_1^S(\mathbf{b}_1^{(l)}) + \mathbf{a}_1^{R-}(\mathbf{b}_1^{(l+1)} - \mathbf{b}_1^{(0)}))] , \quad (14)$$

converging to the sought \mathbf{b}_1 as l increases. Here, and below, \mathbf{b}_1^{0-} , \mathbf{a}_1^{S-} , and \mathbf{a}_1^{R-} denote \mathbf{b}_1^0 , \mathbf{a}_1^S , and \mathbf{a}_1^R , respectively, computed without the possible constant term arising directly from the source. Hence, for example, $\mathbf{b}_1^0(\mathbf{b}_1^{(l+1)}) - \mathbf{b}_1^0(\mathbf{b}_1^{(0)}) = \mathbf{b}_1^{0-}(\mathbf{b}_1^{(l+1)} - \mathbf{b}_1^{(0)})$. In this case, each $\mathbf{b}_1^{(l)}$, for $l=0,1,\dots$, must also be solved iteratively, with iterates $\mathbf{b}_1^{(l,l')}$ for $l'=0,1,2,\dots$

Starting from $\mathbf{b}_1^{(0,0)} = (\mathbf{I} - \mathbf{R}_1 \cdot \mathbf{Q})^{-1} \cdot [\mathbf{b}_1^0(\mathbf{0}) + \mathbf{R}_1 \cdot (\mathbf{a}_1^0 + \mathbf{a}_1^R(\mathbf{0}))]$, let $\mathbf{b}_1^{(0,l'+1)} = \mathbf{b}_1^{(0,0)} + (\mathbf{I} - \mathbf{R}_1 \cdot \mathbf{Q})^{-1} \cdot [\mathbf{b}_1^{0-}(\mathbf{b}_1^{(0,l')}) + \mathbf{R}_1 \cdot \mathbf{a}_1^{R-}(\mathbf{b}_1^{(0,l')})] = \mathbf{b}_1^{(0,l')} + \Delta \mathbf{b}_1^{(0,l')}$ for $l'=0,1,2,\dots$, where

$$\Delta \mathbf{b}_1^{(0,0)} = (\mathbf{I} - \mathbf{R}_1 \cdot \mathbf{Q})^{-1} \cdot [\mathbf{b}_1^{0-}(\mathbf{b}_1^{(0,0)}) + \mathbf{R}_1 \cdot \mathbf{a}_1^{R-}(\mathbf{b}_1^{(0,0)})] \quad \text{and} \quad (15)$$

$$\Delta \mathbf{b}_1^{(0,l')} = (\mathbf{I} - \mathbf{R}_1 \cdot \mathbf{Q})^{-1} \cdot [\mathbf{b}_1^{0-}(\Delta \mathbf{b}_1^{(0,l'-1)}) + \mathbf{R}_1 \cdot \mathbf{a}_1^{R-}(\Delta \mathbf{b}_1^{(0,l'-1)})] \quad \text{for } l' \geq 1. \quad (16)$$

For $l=0,1,2,\dots$, with $\mathbf{b}_1^{(l+1,-1)} = \mathbf{b}_1^{(l)}$ to define the starting starting $\mathbf{b}_1^{(l+1,0)}$, let

$$\mathbf{b}_1^{(l+1,l'+1)} = \mathbf{b}_1^{(0)} + (\mathbf{I} - \mathbf{R}_1 \cdot \mathbf{Q})^{-1} \cdot [\mathbf{b}_1^{0-}(\mathbf{b}_1^{(l+1,l')}) - \mathbf{b}_1^{(0)} + \mathbf{R}_1 \cdot (\mathbf{a}_1^S(\mathbf{b}_1^{(l)}) + \mathbf{a}_1^{R-}(\mathbf{b}_1^{(l+1,l')}) - \mathbf{b}_1^{(0)})] \quad (17)$$

for $l'=-1,0,1,2,\dots$. With $\mathbf{b}_1^{(l+1,l'+1)} = \mathbf{b}_1^{(l+1,l')} + \Delta \mathbf{b}_1^{(l+1,l')}$,

$$\Delta \mathbf{b}_1^{(l+1,0)} = (\mathbf{I} - \mathbf{R}_1 \cdot \mathbf{Q})^{-1} \cdot [\mathbf{b}_1^{0-}(\mathbf{b}_1^{(l+1,0)} - \mathbf{b}_1^{(l)}) + \mathbf{R}_1 \cdot \mathbf{a}_1^{R-}(\mathbf{b}_1^{(l+1,0)} - \mathbf{b}_1^{(l)})] \quad \text{and} \quad (18)$$

$$\Delta \mathbf{b}_1^{(l+1,l')} = (\mathbf{I} - \mathbf{R}_1 \cdot \mathbf{Q})^{-1} \cdot [\mathbf{b}_1^{0-}(\Delta \mathbf{b}_1^{(l+1,l'-1)}) + \mathbf{R}_1 \cdot \mathbf{a}_1^{R-}(\Delta \mathbf{b}_1^{(l+1,l'-1)})] \quad (19)$$

for $l' \geq 1$. Note that $\mathbf{b}_1^{(1,0)} = \mathbf{b}_1^{(0)} + (\mathbf{I} - \mathbf{R}_1 \cdot \mathbf{Q})^{-1} \cdot \mathbf{R}_1 \cdot \mathbf{a}_1^S(\mathbf{b}_1^{(0)})$, and that $\mathbf{b}_1^{(l+1,0)} = \mathbf{b}_1^{(l)} + (\mathbf{I} - \mathbf{R}_1 \cdot \mathbf{Q})^{-1} \cdot \mathbf{R}_1 \cdot \mathbf{a}_1^{S-}(\mathbf{b}_1^{(l)} - \mathbf{b}_1^{(l-1)})$ for $l=1,2,\dots$, cf. [1, Eqs. (33)-(35)]. It is here, for Eq. (17) with $l' = -1$, that the typically more time-consuming wavenumber integrations with respect to κ appear.

Computation of the resulting pressure field proceeds according to [1, Sec. 3.3] with minor changes. As already mentioned, [1, Eq. (8)] is still valid (with $J_{n,0}$ replacing J_n), [1, Eq. (10)] holds with $n = 1$ immediately outside ring anomaly $j=1,\dots,J$, and Eq. (1) is relevant within ring $n=2,\dots,N_j + 1$ of ring anomaly $j=1,\dots,J$. According to Eq. (7), the incoming waves upon ring anomaly $j=1,2,\dots,J$ now include $\mathbf{a}_{1,j}^R$ instead of $\mathbf{a}_{1,j}^S$ if $j_e(j) \neq 0$. Hence, computation of the field within the ring anomalies may now involve the adapted [1, Appendix A]. The field representation by [1, Eq. (37)] is still valid, with a natural connection to the iterates of the iterative solution procedure. It is easy to adapt the paragraph in [1] which includes [1, Eq. (47)] to the case with nested ring anomalies.

4. PARTIAL WAVES FOR MULTIPLE SCATTERING AMONG INDIVIDUAL RING AND STRIP ANOMALIES

In principle, it is easy to extend [1, Sec. 5] to the case with nested ring anomalies. An addition is that reflection-matrix recursions including restarts with vanishing matrices may now be needed not only for the strip structure, but also for ring anomalies which contain other ring anomalies. The resulting elementary reflection matrices allow transmission of partial waves to and from the included smaller ring anomalies. Note that reflections from a ring anomaly which is included in another ring anomaly $j=1,2,\dots,J$ may subsequently be reflected from the outer part (with an elementary $\bar{\mathbf{R}}_{n,j}$ -matrix) or from the inner part (with an elementary $\mathbf{R}_{n,j}$ -matrix) of the surrounding ring anomaly j .

In [1, Sec. 5], the strips are divided into strip anomalies A, B, C, \dots , with single connection strips in between. A convenient way to *formally* circumvent corresponding ring division, and the mentioned reflection-matrix recursions including restarts, is to use nested ring anomalies with common centre points. This simplifies the ring-anomaly nomenclature. As an example, the outer and inner parts of the ring anomaly j mentioned in the previous paragraph could be defined as two different ring anomalies.

REFERENCES

- [1] S. M. Ivansson, “Multiple sound scattering by combinations of cylindrically symmetric and linearly invariant anomalies,” *J. Theor. Comp. Acoust.*, vol. 32, 2450008 (27 pages), 2024.
- [2] S. M. Ivansson, “Coupled-mode field computations for underwater canyons and ridges,” in *Proceedings of the 7th Underwater Acoustics Conference and Exhibition*, (Kalamata, Greece), pp. 137–144, June 25–30, 2023.
- [3] S. M. Ivansson, “Multiple underwater sound scattering by cylindrically symmetric anomalies,” *J. Acoust. Soc. Am.*, vol. 147, pp. 1429–1440, 2020.
- [4] A. Boström, G. Kristensson, and S. Ström, “Transformation properties of plane, spherical and cylindrical scalar and vector wave functions,” in *Field Representations and Introduction to Scattering* (V. V. Varadan, A. Lakhtakia, and V. K. Varadan, eds.), ch. 4, pp. 165–210, North- Holland, 1991.